THE JOURNAL OF PHYSICAL CHEMISTRY C

Article

pubs.acs.org/JPCC

Green Electroluminescence from Charged Phenothiazine Derivative

Kanagaraj Shanmugasundaram,[†] Madayanad Suresh Subeesh,[†] Chozhidakath Damodharan Sunesh,[†] Ramesh Kumar Chitumalla,[‡] Joonkyung Jang,[‡] and Youngson Choe*[,†]

[†]School of Chemical and Biomolecular Engineering and [‡]Department of Nanoenergy Engineering, Pusan National University, Busan 609-735, Republic of Korea

Supporting Information

ABSTRACT: A novel charged green-emitting organic small molecule, PPP, was synthesized and characterized by thermal, photophysical, electrochemical, and electroluminescence investigations. The theoretical properties of PPP were confirmed by means of computational studies. PPP exhibits a good thermal decomposition temperature of 355 °C. The compound PPP shows positive solvatochromism upon increasing the solvent polarity due to the more polarized excited state arising from the intramolecular charge transfer in the excited state. Solid-state emission of PPP was slightly red-shifted compared to that of its solution emission spectrum, showing the reduced intermolecular interaction in the solid state. Solution-processed LEC devices were fabricated using PPP as a neat light-emitting layer. The fabricated single-component light-emitting electrochemical cell devices exhibited green electroluminescence centered at 530 nm with the CIE coordinates of (0.32, 0.58). Electroluminescent devices operated at very low turn-on voltages reveal a maximum luminance of 499 cd/m^2. These promising results are highly desirable for the development of low-cost lighting devices.

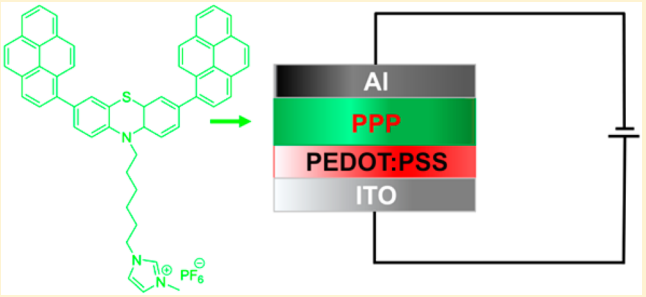

INTRODUCTION

Solid-state fluorescent organic materials have received great interest in recent years owing to their promising functional applications in optoelectronic devices. The pioneering work of Tang and VanSlyke[1] on multilayered organic light-emitting diodes (OLEDs) has reached quite promising levels of performance and is now commercialized even though the manufacturing cost remains a challenge. The multistack OLEDs are constructed by the thermal evaporation of active species under high vacuum. Light-emitting electrochemical cells (LECs) are another category of electroluminescent devices which converts electric current to light within an active layer and are the most anticipated alternative for the aforementioned OLED devices. LECs have several attractive features such as simple device structure and are fabricated from solution under ambient conditions for low-cost electroluminescent devices, as compared to OLEDs.[2−5] The independent work function of electrodes, because the carrier injection is less sensitive, makes LECs more cost-efficient. In LECs, single organic emitters, either neutral conjugated polymer (CP)[6,7] or an ionic transition-metal complex (iTMC),[8−12] enable both ionic and electronic conduction which performs carrier injection upon applied bias.[2,13] These unique potential features make LECs more impressive as compared to OLEDs.

Biscyclometalated iridium(III) complexes are the most utilized material in LEC devices. A huge number of solution-processed high-performance LECs were reported for blue-green, yellow, and red light emission based on ionic iridium(III) complexes.[14−23] Laborious synthesis and purification of polymers hinders device performance.[24] However, the best-performing LECs were reported for conjugated polymers with a blend of ion-conducting polymer and an inorganic salt in the active layer.[7,25] The laborious synthesis of polymers and low abundance and high cost of iridium prevents large-scale, low-cost application of LEC devices. Nowadays considerable attention has been focused on organic small molecules for developing high-performance full-color flat panel displays and solid-state lighting technologies. Therefore, the development of organic small molecules and the endowment of their structural properties are essential for realizing commercially cheaper products. The first solid-state light-emitting electrochemical cells based on organic small molecules were reported by Hill et al.,[26] and the device structure was the same as that of the polymer LECs. Edman and co-workers[3] reported LECs by exploring organic small molecules, and the architecture of the device was same as that of polymer LECs in 2013. More recently, our research group has shown that neutral phenanthroimidazole-based fluorophores are active candidates for solution-processed LECs.[27] In addition to the neutral organic small molecules, to simplify the thin-film architecture, Chen et al. reports LEC devices based on an ionic terfluorene derivative as an active emitter.[28] These results increase great attention to develop charged organic small molecules for low-cost, efficient lighting devices. Recently, solution-processed

Received: May 11, 2016
Revised: August 23, 2016
Published: August 24, 2016

DOI: 10.1021/acs.jpcc.6b04764
J. Phys. Chem. C 2016, 120, 20247−20253

Scheme 1. (i) NaH, 1,6-Dibromohexane, DMF; (ii) NBS, Toluene, AcOH; (iii) $Pd(PPh_3)_4$, TBAB, K_2CO_3, THF/H_2O; (iv) 1-Methylimidazole, Toluene

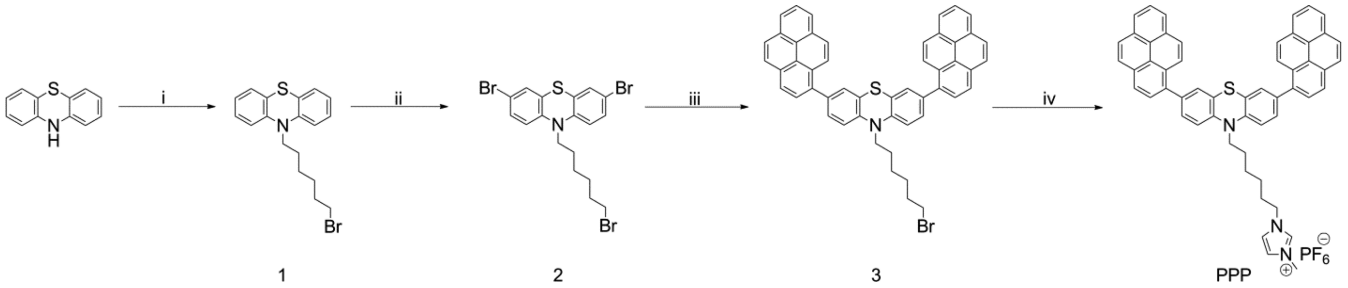

LECs using pure organic small molecules, mostly charged as an efficient material, serve the dual role of charge transport and emitter in the fabricated LECs with efficient emission.[29−36]

Organic materials with multifunctional groups are promising candidates for developing high-performance electroluminescent devices. The beneficial structural entities of pyrene molecules have great attraction because of their rigidity and ordered arrangement in solids. However, planar organic semiconducting materials affect the device performance because of the formation of π-aggregation in the solid thin films. In this regard, phenothiazine had drawn immense research attention because of its strong electron donor nature, and the butterfly conformation prevents molecular aggregation and reduces the intermolecular interactions in solution as well as in the solid state.[37] By encompassing these properties, phenothiazine had wide potential applications in dye-sensitized solar cells,[38] mechanochromism,[39,40] and solid-state lighting applications.[41,42] We have chosen pyrene and phenothiazine entities to build organic semiconducting materials and to explore their favorable properties to evaluate their performance in electroluminescent devices.

In this work, we utilized a phenothiazine−pyrene hybrid design strategy to synthesize the new green emitter PPP, and its photophysical and electroluminescence characteristics were investigated. PPP shows high thermal stability and positive solvatochromism in the emission spectrum due to the intramolecular charge transfer (ICT) in the excited state of the molecule. In particular, solution-processed single-component LECs with PPP as an emitter achieved green light emissions centered at 530 nm with $CIE_{x,y}$ of (0.32, 0.58). The results suggest that the phenothiazine derivatives could be a promising building block for the development of energy-saving full color displays and lighting. This is the first ever study on charged phenothiazine small molecules for constructing electroluminescence devices.

EXPERIMENTAL SECTION

General Information. ^{1}H and ^{13}CNMR spectra were measured with Varian unity Inova-300 MHz spectrometer at room temperature. Purification and a spin coating process were carried out under ambient conditions. Differential scanning calorimetry (DSC) was performed using a TA Instruments Q200 KBSI operated at a heating rate of 10 °C min^{-1}. The glass transition temperature (T_g) was determined from the second heating scan. Thermogravimetric analysis (TGA) was undertaken using a Netzsch TG 209 instrument. The thermal stability of the samples under nitrogen atmosphere was determined by measuring their weight losses while at a heating rate of 20 °C min^{-1}. The ultraviolet−visible (UV−vis) absorption and photoluminescence spectra of the compound were recorded on a UV−vis spectrometer, Lamda-20, PerkinElmer and Hitachi F-7000 FL spectrophotometer, respectively. Photoluminescence quantum yield (PLQY) was measured in dichloromethane solution using 9,10-diphenylanthracene as a standard. The optical band gap (E_g) energy level was obtained from the absorption onset potential. Transient PL measurements were carried out using compact fluorescence lifetime spectrometer C11367 at room temperature. Cyclic voltammetry (CV) measurements were performed on CV model of potentiostat/galvanostat (Iviumstat) voltammetric analyzer with platinum as the working electrode, platinum wire as the counter electrode, and Ag/AgCl as the reference electrode at a scanning rate 100 mV s^{-1}. Tetra-*n*-butylammonium hexafluorophosphate ($TBAPF_6$, 0.10 M) was used as the supporting electrolyte, and acetonitrile was used as the solvent. The experiments were calibrated with the standard ferrocenium/ferrocene (Fc^+/Fc) system. The highest occupied molecular orbital (HOMO) energy level of the molecule calculated from the onset of oxidation potentials using the formula $E_{HOMO} = -4.40 - E_{onset}$ (ox),[43] and the lowest unoccupied molecular orbital (LUMO) was obtained by summing the E_g to the calculated HOMO energy level.

Synthesis. All reagents and solvents used for synthesis were purchased from commercial suppliers and used as received without further purification. The green emitter PPP were designed and synthesized by multistep reactions, as depicted in Scheme 1.

Synthesis of ***1***. A 100 mL three-necked flask was charged with NaH (0.29 g, 12.04 mmol); 30 mL of DMF were stirred for 10 min under an inert atmosphere, and phenothiazine (2.00 g, 10.03 mmol) was added. The resulting mixture was stirred for 30 min. Then 1,6-dibromohexane (1.85 mL, 12.04 mmol) was added, and the mixture was stirred overnight at room temperature. The reaction mixture was quenched with ice−water and extracted with ethyl acetate. The organic fractions were washed with brine solution and dried over Na_2SO_4. After the solvent was removed, the residue was purified by column chromatography on silica gel eluted with *n*-hexane/ethyl acetate (9/1; v/v) to give compound **1** as viscous liquid. Yield: 72%. ^{1}H NMR (300 MHz, $CDCl_3$, δ): 7.22−7.08 (t, 4H), 6.98−6.90 (d, 2H), 6.88−6.78 (d, 2H), 3.85 (t, 2H,), 3.38 (t, 2H,), 1.91−1.74 (m, 4H), 1.54−1.47 (m, 4H).

Synthesis of ***2***. To a solution of compound **1** (2.6 g, 7.17 mmol) in toluene (10 mL) and acetic acid (35 mL) was added *N*-bromosuccinimide (2.68 g, 15.06 mmol) under nitrogen atmosphere. The reaction mixture was stirred at room temperature overnight. The resulting mixture was diluted with water and extracted with dichloromethane. The organic

DOI: 10.1021/acs.jpcc.6b04764
J. Phys. Chem. C 2016, 120, 20247−20253

layer was washed with water and brine, dried over Na_2SO_4, and concentrated under reduced pressure. The crude product was purified by column chromatography on silica gel eluted with hexane to afford compound **2**. Yield: 69%. ^{1}HNMR (300 MHz, $CDCl_3$, δ): 7.36−7.18 (m, 4H), 6.78−6.62 (d, 2H), 3.80 (t, 2H), 3.35 (t, 2H), 1.91−1.66 (m, 4H), 1.51−1.35 (m, 4H).

Synthesis of ***3***. Compound **2** (0.50 g, 0.96 mmol), 1-pyreneboronic acid (0.59 g, 2.40 mmol), $Pd(PPh_3)_4$ (0.04 g, 0.04 mmol), TBAB (0.03 g, 0.10 mmol), and K_2CO_3 (0.66 g, 5.00 mmol) were added to 2:1 (V/V) mixture of tetrahydrofuran/water under argon atmosphere. The reaction mixture was stirred at 70 °C for 24 h. Upon completion of the reaction, the mass was cooled to room temperature; the mixture was extracted with dichloromethane and dried over Na_2SO_4. The solvent was concentrated under reduced pressure, and the residue was purified by column chromatography on silica gel eluted with *n*-hexane/ethyl acetate (9/1; v/v) to afford compound **3** as yellow solid. Yield: 71%. ^{1}H NMR (300 MHz, $CDCl_3$, δ): 8.40−8.15 (m, 8H), 8.15−7.90 (m, 10H), 7.60−7.40 (m, 4H), 7.20−7.05 (s, 2H), 4.10 (t, 2H), 3.45 (t, 2H), 2.10−1.90 (m, 4H), 1.75−1.50 (m, 4H).

Synthesis of PPP. To a solution of compound **3** (0.50 g, 0.65 mmol) in 5 mL toluene was added excess 1-methylimidazole (2 mL), and the resulting reaction mixture was stirred to reflux overnight under argon atmosphere. After completion of the reaction, the mass was concentrated and the final product was obtained by adding saturated KPF_6 solution; the mixture was stirred for 2 h. Then the resulting solid was filtered and washed several times with water and hexane. The product was dried in vacuum at 45 °C for 16 h. The product was purified by recrystallization in DCM with diethyl ether to give target compound PPP. Yield: 76%. ^{1}H NMR (300 MHz, d_6-DMSO, δ): 9.12−9.05 (s, 1H), 8.38−8.24 (m, 6H), 8.23−7.95 (m, 12H), 7.80−7.72 (s, 1H), 7.70−7.64 (s, 1H), 7.54−7.40 (m, 4H), 7.35−7.20 (d, 2H), 4.20 (t, 2H), 4.10 (t, 2H), 3.80 (s, 3H), 1.95−1.75 (m, 4H), 1.60−1.30 (m, 4H). ^{13}C NMR (300 MHz, d_6-DMSO, δ): 144.37, 136.89, 136.37, 135.13, 131.41, 130.84, 130.51, 130.28, 129.17, 128.18, 128.07, 128.01, 127.83, 126.92, 125.85, 125.45, 124.96, 124.62, 124.49, 124.00, 122.69, 116.28, 49.18, 47.10, 36.18, 29.82, 26.66, 26.22, 25.73.

Device Fabrication and Characterization. Indium tin oxide (ITO) coated glass substrates were thoroughly cleaned in an ultrasonic bath of acetone, ethanol, and isopropyl alcohol and dried in an oven at 120 °C. After eing dried, a poly(3,4-ethylenedioxythiophene)-poly(styrenesulfonate) (PEDOT:PSS) layer was spin-coated onto the ITO anode as a buffer layer, and then the sample was dried in a vacuum over 120 °C for an hour. Then the active layer was spin-coated on top of PEDOT/PSS layer, 2 wt % solution in acetonitrile solution followed by annealing at 80 °C for 1 h in vacuum. Sequentially, aluminum cathode contacts were deposited by thermal evaporation at high vacuum through a shadow mask on top of the active layer. Constant voltage scans were used to evaluate the device properties. Electroluminescence spectra and CIE color coordinates were measured using an Avantes luminance spectrum. The current density and luminance versus voltage characteristics were measured using a Keithley 2400 source meter coupled with an OPC 2100 optical spectrum analyzer.

RESULTS AND DISCUSSION

Thermal Properties. Thermal stability of developed material was evaluated by thermal gravimetric analysis and differential scanning calorimetry. The PPP exhibited high thermal decomposition temperatures (T_d) (corresponding to 5% weight loss) of 355 °C, as shown in Figure 1.

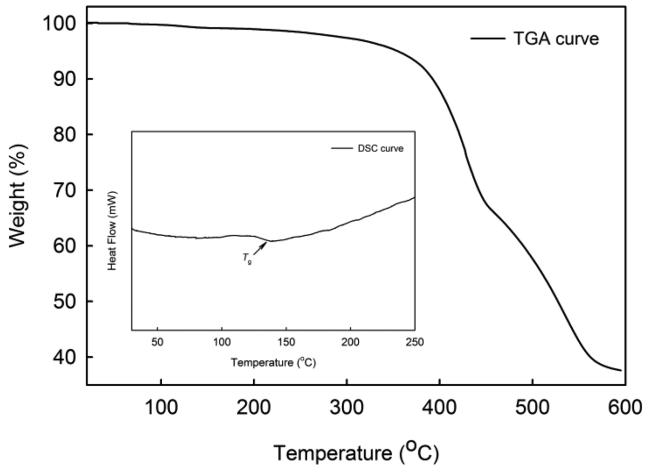

Figure 1. TGA curve (inset: DSC curve) of PPP.

In addition, as shown in Figure 1, the high glass transition temperatures (T_g) of 139 °C was also obtained via differential scanning calorimetry (DSC). High T_g of the molecule arises from the rigidity of the molecular structure which indicates their high morphological stability in the deposited thin films which would benefit the LEC applications. PPP exhibits good thermal stability, which is a highly desired prerequisite for application in organic electroluminescence devices.

Optical Properties. The photophysical properties of PPP were analyzed using ultraviolet−visible and photoluminescence (PL) spectrometers. Figure 2 depicts the UV−vis absorption and photoluminescence spectra of PPP in dilute toluene solution at room temperature. The values are summarized in Table 1.

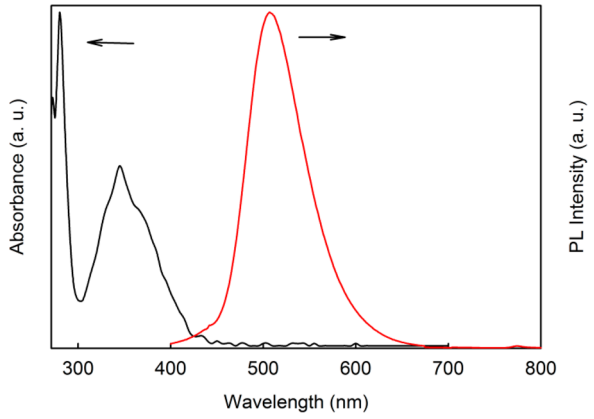

Figure 2. Normalized absorption and PL spectra of PPP in toluene solution.

In the absorption spectrum, compound PPP in toluene solution shows absorption bands around 280 and 345 nm which could be ascribed to the ICT transition and $\pi-\pi^*$ transition of the molecular backbone. The optical energy gap (E_g) of PPP was evaluated from the onset of absorption spectrum of PPP, estimated to be 2.92 eV, which was calculated from the threshold of the absorption spectrum in toluene

DOI: 10.1021/acs.jpcc.6b04764
J. Phys. Chem. C 2016, 120, 20247−20253

Table 1. Photophysical and Thermal Properties of PPP

compound	$\lambda_{UV,max}$[a] (nm)	$\lambda_{PL,max}$[a] (nm)	$\lambda_{UV,max}$[b] (nm)	$\lambda_{PL,max}$[b] (nm)	$\lambda_{PL,max}$[c] (nm)	Φ_f[d]	τ[e] (ns)	E_g[f] (eV)	T_d[g] (°C)
PPP	345	507	349	514	531	0.10/0.03	1.15	2.92	355

[a]Measured in toluene (10^{-5} M) solution. [b]Measured in film state. [c]Measured in solid state. [d]Photoluminescence quantum yield measured in toluene and film state. [e]Lifetime of fluorescence as determined in an oxygen-free toluene solution. [f]Optical band gap as determined from onset of absorption edge. [g]Thermal decomposition (T_d) temperature.

solution. The compound was excited at its maximum absorption and exhibited emission peak around 507 nm in toluene solution. In addition, the fluorescence quantum yield of PPP was measured to be 0.10 in toluene solution using 9,10-diphenylanthracene as a standard (Φ_f = 0.90 in cyclohexane).[44] Thin-film absorption and photoluminescence spectra of PPP were measured and are shown in Figure S3. The thin-film fluorescence spectrum of PPP was slightly red-shifted up to 7 nm as compared to its toluene spectrum. The fluorescence quantum yield of PPP in neat film was measured to be 0.03. UV−vis and PL spectra of PPP were measured in dichloromethane solution and are shown in Figure S4. The absorption bands were similar to that of the bands observed in toluene solution, whereas the emission spectrum in dichloromethane solution was shifted to longer wavelength. The quantum yield of PPP was gradually decreased from 0.10 in toluene (507 nm) to 0.07 in dichloromethane (528 nm). This behavior of the molecule was due to the stabilization of the excited state by solvent molecules, and relaxation occurs through the charge-transfer state radiatively or nonradiatively.[36] Figure S5 shows the transient PL spectrum of PPP in an oxygen-free toluene solution. The compound shows fluorescence lifetime (τ) of 1.15 ns. The solvatochromic behaviors were examined in different solvents with different polarities. PPP exhibited positive solvatochromism upon increasing the polarity of the solvents (Figure S6), showing the intramolecular charge transfer in the excited state. The examined result shows positive solvatochromism with broad red-shifted emissions upon increasing the polarity of the solvent, which shows the sensitivity of the compound to the solvent's polarity. In general, such a broad and structureless pattern of the molecule was attributed to the electronic perturbations by charge transfer or structural reorganization.[37,45] PPP exhibits large Stokes shift in polar solvents up to 83 nm indicating the presence of dipolar nature in the excited state of the compound. The reason for this positive Stokes shift in compound PPP was assigned to the dominant role of intramolecular charge transfer from the strong donor phenothiazine ring to acceptor pyrene molecules.

As shown in Figure 3, the solid-state emission spectrum of compound PPP shows a featureless emission band located at 530 nm. The PL spectrum of the solid was shifted to longer wavelength compared to its thin-film spectrum, indicating the less pronounced self-aggregation of the molecules in the solid state arising from the intermolecular interactions. The phenothiazine-linked compound was not planar, which would efficiently prevent the intermolecular interactions. These results highly suggest that the molecule PPP is most suitable to be used as emitting material in single-component electroluminescent devices.

Electrochemical Properties. Electrochemical behaviors of PPP were investigated by cyclic voltammetry to measure the HOMO levels of the PPP. The oxidation potential of PPP was measured in acetonitrile solution containing tetra-butylammonium hexafluorophosphate as supporting electrolyte, as shown in Figure 4.

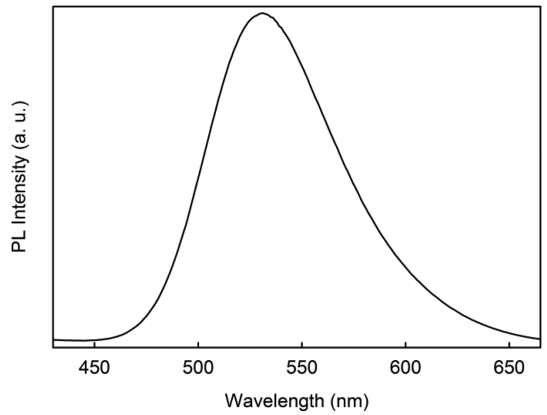

Figure 3. Solid PL spectrum of PPP.

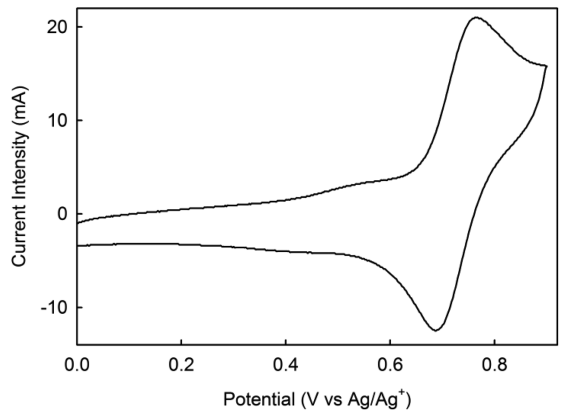

Figure 4. Cyclic voltammogram of PPP.

The HOMO level was estimated from the onset of oxidation curves to be −5.03 eV for compound PPP. This HOMO level suggest that the compound has a good hole-injection ability due to strong electron-donating ability of phenothiazine.[45,46] During negative scan, no reduction peaks were observed for PPP in CV measurements. The absence of reduction potential would affect the n-doping during the operation of LECs. So the LUMO energy levels were calculated by summing the HOMO and the energy gaps (E_g) determined from their absorption edges of the solution UV−vis spectrum. The estimated LUMO level was found to be −2.11 eV.

Theoretical Investigations. To gain further insight into the electronic structure of PPP, density functional theory (DFT) calculations were performed at the B3LYP/6-31G (d) level.[47,48] Figure S7 shows the optimized geometry of PPP. The molecule has nonplanar geometry with a butterfly shape. The bond angles at sulfur (99.4°) and nitrogen (121.7°) were in good agreement with the previously reported results.[49] The methyl group on the imidazole and the counterion (PF_6^-) was not included in the simulations to avoid complexity. Figure 5 depicts the electrochemical comparison of experimental and

DOI: 10.1021/acs.jpcc.6b04764
J. Phys. Chem. C 2016, 120, 20247−20253

theoretical data, as well as the electron density distribution in the frontier molecular orbitals of the compound.

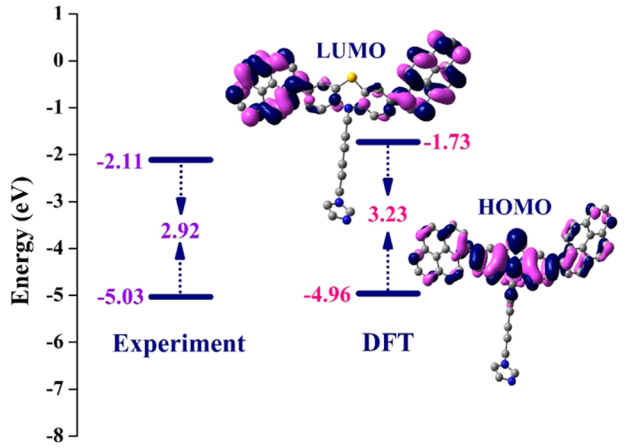

Figure 5. Comparison of experimental and theoretical electrochemical data. Electron density distribution of HOMO and LUMOs.

The electron densities of HOMO and LUMO energy levels were dominantly located on phenothiazine and pyrene rings. The alkyl chain and imidazole ring have no role in the electron density contour plots. The HOMO and LUMO energies of PPP were calculated as −4.96 and −1.73 eV, which were similar to experimentally obtained values. TDDFT were performed at CAM-B3LYP[5]/6-31G(d) level to obtain the UV−vis absorption spectrum of the PPP. To obtain the electronic absorption spectrum, the experimental dichloromethane solution was mimicked by using the polarizable continuum model.[50,51] Figure S8 shows absorption spectrum, and the data are listed in Table S1. As shown in Figure S8, it can be seen that the TDDFT simulations reproduced the main bands that were observed in the experimental absorption spectrum. The simulated low-energy absorption peaks were observed at 351 nm, which were in good agreement with experimental absorption maxima at 345 nm. The low-energy absorption occurred predominantly because of the transitions from HOMO to LUMO (57%).

Electroluminescence Properties. To evaluate the electroluminescence (EL) performance of PPP, single-component single-layered LECs were fabricated with a configuration of ITO/PEDOT:PSS/active layer/Al, in which ITO and Al were used as anode and cathode, respectively. Active layer was spin coated from acetonitrile solution under ambient conditions. The fabricated LEC devices were subjected to a Keithley 2400 source meter to determine LEC device performance.

Figure 6 depicts the green electroluminescence spectrum of PPP in single-layered LECs. The single-component LECs exhibited green EL with maximum at 530 nm with the CIE coordinates of (0.32, 0.58) for PPP. The electroluminescence emission of PPP can be assigned to its intramolecular charge-transfer excited states. The obtained result shows that the electroluminescence spectrum of the compound was red-shifted up to 15 nm compared to its thin-film PL spectrum, which arises from intermolecular interaction of the molecules in the solid state. However, green light emission is of interest to construct white light-emitting devices by blending of red−green−blue emitters in light-emitting devices.[52] Figure 7 shows the time-independent brightness (L−V) and current density (J−V) plots of the single-layered LEC devices. The devices

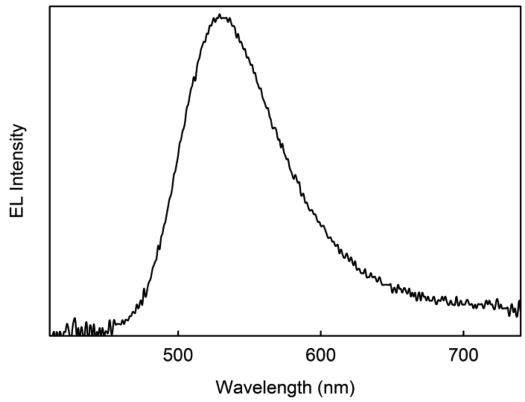

Figure 6. Electroluminescence spectrum of PPP.

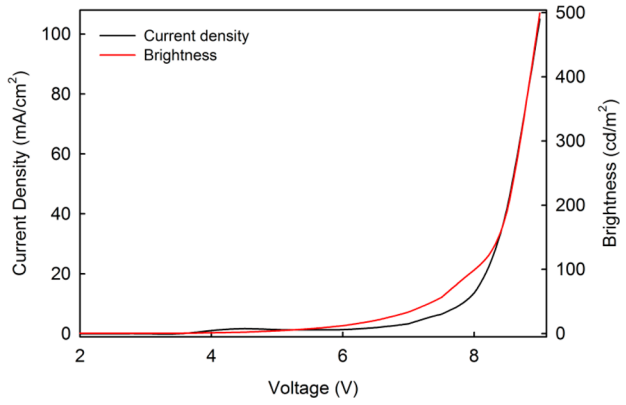

Figure 7. Current density−voltage−luminescence (J−V−L) characteristics of LECs based on PPP.

were investigated by voltage scanning with a sweep rate of 0.5 V/s. It should be noted that PPP-based LEC devices exhibited the low turn-on voltage (Figure S9) of 4.0 V (at B > 1 cd/m^2), maximum brightness of 499 cd/m^2, and maximum current density of 105 mA/cm^2 at 9.0 V.

The attainment of such a low turn-on voltage and maximum brightness at 9.0 V in a solution-processed LEC device shows the charge-transporting ability of PPP due to the D−A character of the compound.[46] The low turn-on voltage depends on the lower injection barrier and charge-transfer phenomena of the material. In comparison to the previously reported nonionic small molecule, PPP shows reasonable performances in terms of brightness.[3] However, the observed results demonstrate the potential of an ionic phenothiazine derivative as green emitter in single-layered LECs.

CONCLUSIONS

We have designed and synthesized a new green light-emitting molecule, PPP, containing electron-donating phenothiazine and electron-accepting pyrene cores. The synthesized compound was intrinsically ionic to mediate the charge transport in single-layered electroluminescence devices. Thermal, photophysical, electrochemical, and electroluminescence characteristics of PPP were investigated. The geometrical, electronic, and optical properties of the compound were obtained by employing DFT and TDDFT studies. Compound PPP exhibited a high decomposition temperature of 355 °C. Large solvatochromism was exhibited in solution because of the strong intramolecular charge transfer in the molecule. The observed thin-film

DOI: 10.1021/acs.jpcc.6b04764
J. Phys. Chem. C 2016, 120, 20247−20253

photoluminescence spectra were shifted to longer wavelength than that of solution PL spectra, which arises from the intermolecular interaction in the solid state. The single-component single-layered LEC devices show green electroluminescence centered at 530 nm, which is similar to its solid PL spectra with the CIE coordinates of (0.32, 0.58). The LEC device shows low turn-on voltage of 4.0 V and maximum brightness of 499 cd/m^2 at 9.0 V. A detailed investigation is in progress toward improving the electroluminescence device performance.

■ ASSOCIATED CONTENT

Supporting Information

The Supporting Information is available free of charge on the ACS Publications website at DOI: 10.1021/acs.jpcc.6b04764.

^{1}H NMR spectrum of PPP; ^{13}C NMR spectrum of PPP; UV−vis absorption spectrum of PPP in thin films; UV−vis absorption spectrum of PPP in DCM solution; transient PL spectrum of PPP in an oxygen-free toluene solution; PL spectrum in different solvents; DFT-optimized ground-state geometry of the compound PPP; UV−vis absorption spectrum of PPP simulated in dichloromethane; turn-on voltage of LEC device in higher magnification; results of TDDFT calculations (PDF)

■ AUTHOR INFORMATION

Corresponding Author

*E-mail: choe@pusan.ac.kr. Tel.: +8251 510 2396. Fax: +8251 512 8634.

Notes

The authors declare no competing financial interest.

■ ACKNOWLEDGMENTS

This research work has been supported by Basic Science Research program through National Research Foundation of Korea (NRF) financial support by Ministry of Education, Science and Technology (NRF-2013R1A1A4A03009795) and Brain Korea 21 Plus project.

■ REFERENCES

(1) Tang, C. W.; VanSlyke, S. A. Organic Electroluminescent Diodes. *Appl. Phys. Lett.* **1987**, *51*, 913−915.

(2) Pei, Q.; Yu, G.; Zhang, C.; Yang, Y.; Heeger, A. J. Polymer Light-Emitting Electrochemical cells. *Science* **1995**, *269*, 1086−1088.

(3) Tang, S.; Tan, W.-Y.; Zhu, X.-H.; Edman, L. Small-Molecule Light-Emitting Electrochemical Cells: Evidence for in Situ Electrochemical Doping and Functional Operation. *Chem. Commun.* **2013**, *49*, 4926−4928.

(4) Tang, S.; Buchholz, H. A.; Edman, L. White Light from a Light-Emitting Electrochemical Cell: Controlling the Energy-Transfer in a Conjugated Polymer/Triplet-Emitter Blend. *ACS Appl. Mater. Interfaces* **2015**, *7*, 25955−25960.

(5) Mindemark, J.; Edman, L. Illuminating the Electrolyte in Light-Emitting Electrochemical Cells. *J. Mater. Chem. C* **2016**, *4*, 420−432.

(6) Pei, Q.; Yang, Y.; Yu, G.; Zhang, C.; Heeger, A. J. Polymer Light-Emitting Electrochemical Cells: In situ Formation of a Light-Emitting p-n Junction. *J. Am. Chem. Soc.* **1996**, *118*, 3922−3929.

(7) Hernandez-Sosa, G.; Eckstein, R.; Tekoglu, S.; Becker, T.; Mathies, F.; Lemmer, U.; Mechau, N. The Role of the Polymer Solid Electrolyte Molecular Weight in Light-Emitting Electrochemical Cells. *Org. Electron.* **2013**, *14*, 2223−2227.

(8) Costa, R. D.; Orti, E.; Bolink, H. J.; Monti, F.; Accorsi, G.; Armaroli, N. Luminescent Ionic Transition-Metal Complexes for Light-Emitting Electrochemical Cells. *Angew. Chem., Int. Ed.* **2012**, *51*, 8178−8211.

(9) Lyons, C. H.; Abbas, E. D.; Lee, J.-K.; Rubner, M. F. Solid-State Light-Emitting Devices Based on the Trischelated Ruthenium(II) Complex. 1. Thin Film Blends with Poly(ethylene oxide). *J. Am. Chem. Soc.* **1998**, *120*, 12100−12107.

(10) Handy, E. S.; Pal, A. J.; Rubner, M. F. Solid-State Light-Emitting Devices Based on the Tris-Chelated Ruthenium(II) Complex. 2. Tris(bipyridyl)ruthenium(II) as a High-Brightness Emitter. *J. Am. Chem. Soc.* **1999**, *121*, 3525−3528.

(11) Gonzalez, I.; Dreyse, P.; Cortes-Arriagada, D.; Sundararajan, M.; Morgado, C.; Brito, I.; Roldan-Carmona, C.; Bolink, H. J.; Loeb, B. A Comparative Study of Ir(III) Complexes with Pyrazino[2,3-*f*][1,10]-Phenanthroline and Pyrazino[2,3-*f*][4,7]Phenanthroline Ligands in Light-Emitting Electrochemical Cells (LECs). *Dalton Trans.* **2015**, *44*, 14771−14781.

(12) Sunesh, C. D.; Mathai, G.; Choe, Y. Green and Blue-Green Light-Emitting Electrochemical Cells Based on Cationic Iridium Complexes with 2-(4-ethyl-2-pyridyl)-1H-imidazole Ancillary Ligand. *Org. Electron.* **2014**, *15*, 667−674.

(13) Van Reenen, S.; Matyba, P.; Dzwilewski, A.; Janssen, R. A. J.; Edman, L.; Kemerink, M. A. A Unifying Model for the Operation of Light-Emitting Electrochemical Cells. *J. Am. Chem. Soc.* **2010**, *132*, 13776−13781.

(14) Sunesh, C. D.; Shanmugasundaram, K.; Subeesh, M. S.; Chitumalla, R. K.; Jang, J.; Choe, Y. Blue and Blue-Green Light-Emitting Cationic Iridium Complexes: Synthesis, Characterization, and Optoelectronic Properties. *ACS Appl. Mater. Interfaces* **2015**, *7*, 7741−7751.

(15) Yang, C.-H.; Mauro, M.; Polo, F.; Watanabe, S.; Muenster, I.; Fröhlich, R.; De Cola, L. Deep-Blue-Emitting Heteroleptic Iridium(III) Complexes Suited for Highly Efficient Phosphorescent OLEDs. *Chem. Mater.* **2012**, *24*, 3684−3695.

(16) He, L.; Qiao, J.; Duan, L.; Dong, G. F.; Zhang, D. Q.; Wang, L. D.; Qiu, Y. Toward Highly Efficient Solid-State White Light-Emitting Electrochemical Cells: Blue-Green to Red Emitting Cationic Iridium Complexes with Imidazole Type Ancillary Ligands. *Adv. Funct. Mater.* **2009**, *19*, 2950−2960.

(17) Hu, T.; He, L.; Duan, L.; Qiu, Y. Solid-State Light-Emitting Electrochemical Cells Based on Ionic Iridium(III) Complexes. *J. Mater. Chem.* **2012**, *22*, 4206−4215.

(18) Sunesh, C. D.; Mathai, G.; Choe, Y. Constructive Effects of Long Alkyl Chains on the Electroluminescent Properties of Cationic Iridium Complex-Based Light-Emitting Electrochemical Cells. *ACS Appl. Mater. Interfaces* **2014**, *6*, 17416−17425.

(19) Su, H. C.; Wu, C. C.; Fang, F. C.; Wong, K. T. Efficient Solid-State Host-Guest Light-Emitting Electrochemical Cells Based on Cationic Transition Metal Complexes. *Appl. Phys. Lett.* **2006**, *89*, 261118−261121.

(20) Costa, R. D.; Orti, E.; Bolink, H. J.; Graber, S.; Schaffner, S.; Neuburger, M.; Housecroft, C. E.; Constable, E. C. Archetype Cationic Iridium Complexes and Their Use in Solid-State Light-Emitting Electrochemical Cells. *Adv. Funct. Mater.* **2009**, *19*, 3456−3463.

(21) Tamayo, A. B.; Garon, S.; Sajoto, T.; Djurovich, P. I.; Tsyba, I. M.; Bau, R.; Thompson, M. E. Cationic Bis-cyclometalated Iridium(III) Diimine Complexes and Their Use in Efficient Blue, Green, and Red Electroluminescent Devices. *Inorg. Chem.* **2005**, *44*, 8723−8732.

(22) Liao, C.-T.; Chen, H.-F.; Su, H.-C.; Wong, K.-T. Tailoring Carrier Injection Efficiency to Improve the Carrier Balance of Solid-State Light-Emitting Electrochemical Cells. *Phys. Chem. Chem. Phys.* **2012**, *14*, 9774−9784.

(23) Costa, R. D.; Cespedes-Guirao, F. J.; Orti, E.; Bolink, H. J.; Gierschner, J.; Fernandez-Lazaro, F.; Sastre-Santos, A. Efficient Deep-Red Light-Emitting Electrochemical Cells Based on a Perylenediimide-Iridium-Complex Dyad. *Chem. Commun.* **2009**, 3886−3888.

(24) Scherf, U.; List, E. J. W. Semiconducting Polyfluorenes-Towards Reliable Structure-Property Relationships. *Adv. Mater.* **2002**, *14*, 477−487.

DOI: 10.1021/acs.jpcc.6b04764
J. Phys. Chem. C 2016, 120, 20247−20253

(25) Sandström, A.; Dam, H. F.; Krebs, F. C.; Edman, L. Ambient Fabrication of Flexible and Large-Area Organic Light-Emitting Devices Using Slot-Die Coating. *Nat. Commun.* **2012**, *3*, 1002−1006.
(26) Hill, Z. B.; Rodovsky, D. B.; Leger, J. M.; Bartholomew, G. P. Synthesis and Utilization of Perylene-Based *n*-Type Small Molecules in Light-Emitting Electrochemical Cells. *Chem. Commun.* **2008**, 6594−6596.
(27) Subeesh, M. S.; Shanmugasundaram, K.; Sunesh, C. D.; Won, Y. S.; Choe, Y. Utilization of a Phenanthroimidazole Based Fluorophore in Light-Emitting Electrochemical Cells. *J. Mater. Chem. C* **2015**, *3*, 4683−4687.
(28) Chen, H.-F.; Liao, C.-T.; Chen, T.-C.; Su, H.-C.; Wong, K.-T.; Guo, T.-F. An Ionic Terfluorene Derivative for Saturated Deep-Blue Solid State Light-Emitting Electrochemical Cells. *J. Mater. Chem.* **2011**, *21*, 4175−4181.
(29) Chen, H.-F.; Liao, C.-T.; Kuo, M.-C.; Yeh, Y.-S.; Su, H.-C.; Wong, K.-T. UV Light-Emitting Electrochemical Cells Based on an Ionic 2,2′ -Bifluorene Derivative. *Org. Electron.* **2012**, *13*, 1765−1773.
(30) Pertegás, A.; Tordera, D.; Serrano-Pérez, J. J.; Ortí, E.; Bolink, H. J. Light-emitting electrochemical cells using cyanine dyes as the active components. *J. Am. Chem. Soc.* **2013**, *135*, 18008−18011.
(31) Pertegás, A.; Shavaleev, N. M.; Tordera, D.; Ortí, E.; Nazeeruddin, M. K.; Bolink, H. J. Host-Guest Blue Light-Emitting Electrochemical Cells. *J. Mater. Chem. C* **2014**, *2*, 1605−1611.
(32) Wong, M. Y.; Hedley, G. J.; Xie, G.; Kölln, L. S.; Samuel, I. D. W.; Pertegás, A.; Bolink, H. J.; Zysman-Colman, E. Light-Emitting Electrochemical Cells and Solution-Processed Organic Light-Emitting Diodes Using Small Molecule Organic Thermally Activated Delayed Fluorescence Emitters. *Chem. Mater.* **2015**, *27*, 6535−6542.
(33) Shanmugasundaram, K.; Subeesh, M. S.; Sunesh, C. D.; Chitumalla, R. K.; Jang, J.; Choe, Y. Synthesis and Photophysical Characterization of an Ionic Fluorene Derivative for Blue Light-Emitting Electrochemical Cells. *Org. Electron.* **2015**, *24*, 297−302.
(34) Subeesh, M. S.; Shanmugasundaram, K.; Sunesh, C. D.; Nguyen, T. P.; Choe, Y. Phenanthroimidazole Derivative as an Easily Accessible Emitter for Non-Doped Light-Emitting Electrochemical Cells. *J. Phys. Chem. C* **2015**, *119*, 23676−23684.
(35) Shanmugasundaram, K.; Subeesh, M. S.; Sunesh, C. D.; Choe, Y. Non-Doped Deep Blue Light-Emitting Electrochemical Cells from Charged Organic Small Molecules. *RSC Adv.* **2016**, *6*, 28912−28918.
(36) Subeesh, M. S.; Shanmugasundaram, K.; Sunesh, C. D.; Chitumalla, R. K.; Jang, J.; Choe, Y. Host-Dopant System to Generate Bright Electroluminescence from Small Organic Molecule Functionalized Light-Emitting Electrochemical Cells. *J. Phys. Chem. C* **2016**, *120*, 12207−12217.
(37) Konidena, R. K.; Thomas, K. R. J.; Kumar, S.; Wang, Y.-C.; Li, C.-J.; Jou, J.-H. Phenothiazine Decorated Carbazoles: Effect of Substitution Pattern on the Optical and Electroluminescent Characteristics. *J. Org. Chem.* **2015**, *80*, 5812−5823.
(38) Hua, Y.; Chang, S.; Huang, D.; Zhou, X.; Zhu, X.; Zhao, J.; Chen, T.; Wong, W.-Y.; Wong, W.-K. Significant Improvement of Dye-Sensitized Solar Cell Performance Using Simple Phenothiazine-Based Dyes. *Chem. Mater.* **2013**, *25*, 2146−2153.
(39) Xue, P.; Yao, B.; Liu, X.; Sun, J.; Gong, P.; Zhang, Z.; Qian, C.; Zhang, Y.; Lu, R. Reversible Mechanochromic Luminescence of Phenothiazine-Based 10,10;-Bianthracene Derivatives with Different Lengths of Alkyl Chains. *J. Mater. Chem. C* **2015**, *3*, 1018−1025.
(40) Zhang, G.; Sun, J.; Xue, P.; Zhang, Z.; Gong, P.; Peng, J.; Lu, R. Phenothiazine Modified Triphenylacrylonitrile Derivatives: AIE and Mechanochromism Tuned by Molecular Conformation. *J. Mater. Chem. C* **2015**, *3*, 2925−2932.
(41) Bodedla, G. B.; Thomas, K. R. J.; Kumar, S.; Jou, J.-H.; Li, C.-J. Phenothiazine-Based Bipolar Green-Emitters Containing Benzimidazole Units: Synthesis, Photophysical and Electroluminescence Properties. *RSC Adv.* **2015**, *5*, 87416−87428.
(42) Lee, I. H.; Lee, J. Y. Phenothiazine Dioxide Based High Triplet Energy Host Materials for Blue Phosphorescent Organic Light-Emitting Diodes. *RSC Adv.* **2015**, *5*, 97903−97909.
(43) Kulkarni, A. P.; Tonzola, C. J.; Babel, A.; Jenekhe, S. S. Electron Transport Materials for Organic Light-Emitting Diodes. *Chem. Mater.* **2004**, *16*, 4556−4573.
(44) Reddy, S. S.; Sree, V. G.; Gunasekar, K.; Cho, W.; Gal, Y.-S.; Song, M.; Kang, J.-W.; Jin, S.-H. Highly Efficient Bipolar Deep-Blue Fluorescent Emitters for Solution-Processed Non-doped Organic Light-Emitting Diodes Based on 9,9-Dimethyl-9,10- dihydroacridine/Phenanthroimadazole Derivatives. *Adv. Opt. Mater.* **2016**, *4*, 1236.
(45) Jenekhe, S. A.; Lu, L.; Alam, M. M. New Conjugated Polymers with Donor-Acceptor Architectures: Synthesis and Photophysics of Carbazole-Quinoline and Phenothiazine-Quinoline Copolymers and Oligomers Exhibiting Large Intramolecular Charge Transfer. *Macromolecules* **2001**, *34*, 7315−7324.
(46) Kulkarni, A. P.; Kong, X.; Jenekhe, S. A. High-Performance Organic Light-Emitting Diodes Based on Intramolecular Charge-Transfer Emission from Donor-Acceptor Molecules: Significance of Electron-Donor Strength and Molecular Geometry. *Adv. Funct. Mater.* **2006**, *16*, 1057−1066.
(47) Becke, A. D. Density-Functional Thermochemistry. III. The Role of Exact Exchange. *J. Chem. Phys.* **1993**, *98*, 5648−5652.
(48) Becke, A. D. Density-Functional Thermochemistry. IV. A New Dynamical Correlation Functional and Implications for Exact-Exchange Mixing. *J. Chem. Phys.* **1996**, *104*, 1040−1046.
(49) Yao, L.; Sun, S.; Xue, S.; Zhang, S.; Wu, X.; Zhang, H.; Pan, Y.; Gu, C.; Li, F.; Ma, Y. Aromatic S-Heterocycle and Fluorene Derivatives as Solution-Processed Blue Fluorescent Emitters: Structure−Property Relationships for Different Sulfur Oxidation States. *J. Phys. Chem. C* **2013**, *117*, 14189−14196.
(50) Miertuš, S.; Scrocco, E.; Tomasi, J. Electrostatic Interaction of a Solute with a Continuum. A Direct Utilizaion of AB Initio Molecular Potentials for the Prevision of Solvent Effects. *Chem. Phys.* **1981**, *55*, 117−129.
(51) Cossi, M.; Barone, V.; Cammi, R.; Tomasi, J. Ab Initio Study of Solvated Molecules: a New Implementation of the Polarizable Continuum Model. *Chem. Phys. Lett.* **1996**, *255*, 327−335.
(52) Akatsuka, T.; Roldan-Carmona, C.; Orti, E.; Bolink, H. J. Dynamically Doped White Light Emitting Tandem Devices. *Adv. Mater.* **2014**, *26*, 770−774.

DOI: 10.1021/acs.jpcc.6b04764
J. Phys. Chem. C 2016, 120, 20247−20253